



Reinvestigation and superstructure of $\text{La}_{3.67}[\text{Fe}(\text{C}_2)_3]$

Bambar Davaasuren, Enkhtsetseg Dashjav, Guido Kreiner, Horst Borrmann, Rüdiger Kniep*

Max-Planck-Institut für Chemische Physik fester Stoffe, Nöthnitzer Str. 40, 01187 Dresden, Germany

ARTICLE INFO

Article history:

Received 22 July 2008

Received in revised form

12 January 2009

Accepted 28 January 2009

Available online 6 February 2009

Keywords:

Ternary carbides

Rare-earth compounds

Crystal structure

Superstructure

ABSTRACT

The lanthanum iron carbide $\text{La}_{3.67}[\text{Fe}(\text{C}_2)_3]$ was prepared from the elements by argon arc-melting followed by annealing. The crystal structure of the ternary phase was reported previously (space group $P6_3/m$ with $a = 878.7(2)$ pm, and $c = 535.1(1)$ pm) [A.M. Witte, W. Jeitschko, Z. Naturforsch. 51b (1996) 249–255]. In the present work the compound was reinvestigated by X-ray powder and single crystal diffraction, and was further characterized by metallographic methods and chemical analyses. Our diffraction data clearly reveal a superstructure with weak superstructure reflections in the space group $P6_3/m$ with $a = 879.26(8)$ pm and $c = 1604.59(15)$ pm, thus tripling the previously reported subcell. The crystal structure (refinement to $R1 = 0.044$ and $wR2 = 0.075$ for 1387 unique reflections and 60 variables) contains $\text{Fe}(\text{C}_2)_3$ trigonal planar groups with the C_2 ligands bonded end-on to the Fe atoms. The C–C distance is typical for a double bond. La atoms as the least electronegative component surround the complex anions and form a framework of face-sharing tricapped trigonal prisms. The resulting hexagonal channels at 0, 0, z of the partial structure with chemical composition La_3FeC_6 are occupied by four additional La atoms per unit cell. These La atoms are fully ordered within a linear chain and display a Peierls-like distortion pattern. However, no long-range order in the a – b plane has been observed due to the random orientation of the chains. Because of the two different orientations which are possible for each chain the situation is similar to an Ising model on a triangular lattice.

Crown Copyright © 2009 Published by Elsevier Inc. All rights reserved.

1. Introduction

Recently, the family of ternary carbides $RE_xT_yC_z$ (RE = rare-earth metals or actinoids; T = transition metals; C = monoatomic C^{4-} species) has been classified into two groups according to structural characteristics and the ratio $(x+y)/z$, i.e., carbometalates with $(x+y)/z \leq 2$ containing complex anions and metal-rich carbides with $(x+y)/z \geq 4$ [2]. In the search for novel carbometalates we also explored the systems RE – Fe – C . Compounds of this type have been proposed as potential hard magnet materials [3]. In spite of intensive explorations of the respective phase diagrams only a few compounds with $(x+y)/z < 2$ have been reported: $RE_2\text{FeC}_4$ ($RE = \text{Y}, \text{Tb}–\text{Lu}$) [4], Sc_3FeC_4 [5], $RE\text{FeC}_2$ [6], ScFeC_2 [7] and $RE_{3.67}\text{FeC}_6$ ($RE = \text{La}–\text{Nd}, \text{Sm}$) [1]. All these compounds contain C_2 -pairs as structural units instead of monoatomic carbon ligands, thus, in a strict sense they do not belong to the class of carbometalates. During our recent work in the system $\text{La}–\text{Fe}–\text{C}$ we reinvestigated the crystal structure of $\text{La}_{3.67}\text{FeC}_6$, which had been described already in a previous communication by Witte and Jeitschko [1]. In the present work we report on the determination of a superstructure of this compound.

2. Experimental

2.1. Preparation

All handlings were carried out in a glove box under argon atmosphere (MBraun, $p(\text{O}_2, \text{H}_2\text{O}) < 1$ ppm). The title compound was prepared by arc-melting of cold pressed pellets of La (Ames, 99.99%), Fe (Alfa Aesar, 99.99%) and graphitic carbon (Chempur, 99.9%) in the molar ratios 3:1:6 and 3.67:1:6. The button specimens of about 0.6 g total mass were remelted several times to ensure compositional homogeneity. The samples were then wrapped in Fe-foils, which in turn were encapsulated in fused silica tubes, heat treated at 1173 K for 21 days, and finally quenched in cold water. The reaction products were gray with metallic luster.

2.2. Phase analysis and crystal structure determination

Powder XRD data were collected on a Huber Guinier camera G670 (transmission geometry, $\text{CoK}\alpha_1$ radiation ($\lambda = 178.896(1)$ pm), primary-beam $\text{Ge}(111)$ monochromator, flat sample holder with vaseline-coated Mylar foil, LaB_6 as internal standard). Continuous scan data were collected in the range $10^\circ < 2\theta < 85^\circ$ with a step width of 0.005° . According to powder X-ray diffraction analyses the title compound was the majority phase in all samples

* Corresponding author. Fax: +49 351 4646 3002.

E-mail address: kniep@cpfs.mpg.de (R. Kniep).

(Fig. 1) and only a small number of very weak reflections originating from a minority phase with unknown crystal structure were observed. The unit cell parameters of the hexagonal structure ($a = 879.26(8)$ pm and $c = 1604.59(15)$ pm) were determined by least-squares refinement of the peak positions using the program WinXpow [8].

For metallographic examination pieces of about 5 mm in diameter were embedded in epoxy resin. Grinding was performed using fixed abrasive papers (SiC, grain sizes 45, 20 and 10 μm) and paraffin oil as lubricant. Polishing was done in four steps using slurries of 6-, 3-, 1- and $\frac{1}{4}$ -micron diamond powders in paraffin oil. After each step the specimens were cleaned with *n*-hexane to remove all particles and the paraffin oil. The microstructure and the chemical composition of the samples were examined by optical (bright field) and scanning electron microscopy (Zeiss Axioplan 2 and SEM Philips XL 30 with integrated energy dispersive (EDX) spectrometer, respectively). The sample with composition 3.67:1:6 is nearly single phase material of the title compound. Fig. 2 shows a BSE image of a typical microstructure of this sample with large crystals of the title compound. The space between grains of the majority phase is filled by small amounts of an unknown phase. The fine matrix is probably a remnant of a

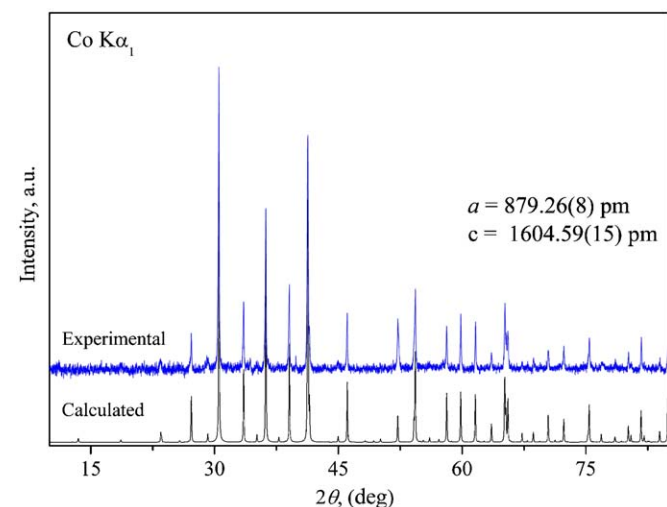


Fig. 1. Experimental and calculated X-ray powder diffraction patterns for $\text{La}_{3.67}[\text{Fe}(\text{C}_2)_3]$.

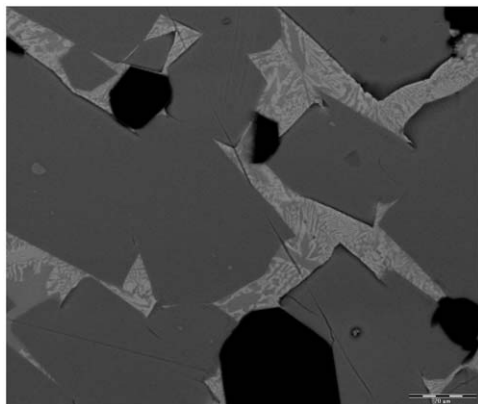


Fig. 2. BSE image of a typical microstructure after prolonged heat treatment; the title compound is the primary phase and the fine matrix in between is composed of the title compound and an unknown phase.

eutectic structure, which has partly survived even the prolonged heat treatments. EDX analyses on selected areas gave an average atomic ratio of La:Fe = 3:1. No reliable determination of the chemical composition of the unknown phase was possible.

Prismatic-shaped single crystals obtained from both compositions were mounted on glass fibers and sealed in glass capillaries. Because of better quality, the crystal from the sample started with 3:1:6 ratio was chosen for intensity data collection. It was carried out on a Rigaku AFC7 diffractometer with Mercury CCD detector and graphite monochromatized $\text{MoK}\alpha$ ($\lambda = 71.069$ pm) radiation. The crystal structure was solved by direct methods and refined using the program packages SHELXS97 and SHELXL97 [9]. Both, powder and single crystal diffraction data clearly reveal a primitive hexagonal cell with weak superstructure reflections arising from a tripled cell along *c*. Relevant crystallographic data and further details of data collection and structure refinement are

Table 1

Crystallographic data and details on data collection and structure refinement for $\text{La}_{3.67}[\text{Fe}(\text{C}_2)_3]$.

Chemical formula	$\text{La}_{3.67}[\text{Fe}(\text{C}_2)_3]$
Crystal system	Hexagonal
Space group	$P6_3/m$ (no. 176)
Formula unit	$Z = 6$
Formula mass/ g mol^{-1}	637.23
Radiation, λ/pm	$\text{MoK}\alpha$, 71.069
Temperature/K	295
<i>a</i> /pm	879.3(2)
<i>b</i> /pm	1605.0(7)
<i>V</i> /pm ³ 10 ⁶	1074.5(6)
$\rho_{\text{calc}}/\text{g cm}^{-3}$	5.909
Crystal size/ μm	$0.20 \times 0.12 \times 0.11$
$T_{\text{min}}, T_{\text{max}}$	0.049, 0.077
R_{int}	0.0414
θ -range/ $^\circ$	2.54–33.79
<i>h k l</i> -range	$-13 \leq h \leq 13$ $-13 \leq k \leq 12$ $-23 \leq l \leq 20$
Extinction coefficient χ^a	0.00030(9)
Absorption correction	Multiscan
Absorption coefficient, μ (mm^{-1})	23.28
Unique reflections/parameters	1387/60
$R(F_o)/R_w(F_o^2)/\text{Goof}$ (all data)	0.044/0.075/1.19
max./min. $\Delta\rho$ [$e^{-}/(10^6 \text{ pm}^3)$]	5.42/−7.45
$w1/w2^b$	0/25.78

Supplementary data for this paper are available from the FIZ, D-76344 Eggenstein-Leopoldshafen, Germany, e-mail crysdata@FIZ-karlsruhe.de, by quoting the depository number 419578.

$$^a F_c \text{ is multiplied by } k[1+0.001 \cdot x F_c^2 \cdot \lambda^3 / \sin(2\theta)]^{-1/4}.$$

$$^b R = \sum ||F_o| - |F_c|| / \sum |F_o|, \quad wR = \sum w(F_o^2 - F_c^2)^2 / (\sum w(F_o^2)^2)^{1/2} \quad \text{with } w = 1/[\sigma^2(F_o^2) + (w1 \cdot P)^2 + w2 \cdot P] \quad \text{with } P = (\max(F_o^2, 0) + 2F_c^2)/3.$$

Table 2

$\text{La}_{3.67}[\text{Fe}(\text{C}_2)_3]$: fractional atomic coordinates and equivalent isotropic displacement parameters [10^4 pm^2]; estimated standard deviations are given in parentheses.

Atom	Site	occ.	x	y	z	U_{eq}
La1	12i		0.39347(5)	0.33437(5)	0.08448(3)	0.00883(12)
La2	6h		0.06318(8)	0.39877(8)	$\frac{1}{4}$	0.00874(15)
La3	4e	$\frac{1}{2}$	0	0	0.02233(9)	0.0102(3)
La4	4e	$\frac{1}{2}$	0	0	0.18995(9)	0.0105(3)
Fe1	4f	$\frac{1}{3}$	$\frac{2}{3}$	$\frac{2}{3}$	0.08260(12)	0.0075(3)
Fe2	2d	$\frac{2}{3}$	$\frac{1}{3}$	$\frac{1}{3}$	$\frac{1}{4}$	0.0086(5)
C1	12i		0.0240(13)	0.2771(13)	0.0849(5)	0.029(2)
C2	12i		0.1475(10)	0.4426(10)	0.0831(5)	0.0118(13)
C3	6h		0.2861(14)	0.2778(15)	$\frac{1}{4}$	0.0103(19)
C4	6h		0.4426(14)	0.2987(14)	$\frac{1}{4}$	0.0074(18)

listed in Table 1. The fractional atomic coordinates and anisotropic displacement parameters are listed in Tables 2 and 3, respectively.

3. Results and discussion

The crystal structure of $\text{La}_{3.67}\text{FeC}_6$ was refined in the space group $P6_3/m$ (176) with residuals $R1 = 0.044$ and $wR2 = 0.075$ for 1387 unique reflections and 60 variables. The atoms are distributed on 4 La, 2 Fe and 4 C sites in the unit cell. The occupancy factors were refined in separate series of least-squares cycles as a check for partial occupancy. The refinement revealed full occupancy for all sites except those of La3 and La4. In the final cycles of the refinement the site occupancy for La3 and La4 was set to 0.5 as a refinement without respective constraints did not reveal deviations beyond the estimated standard deviations.

The crystal structure of $\text{La}_{3.67}\text{FeC}_6$ contains $\text{Fe}(\text{C}_2)_3$ trigonal planar groups (Fig. 3a) with C_2 ligands bonded end-on to the iron atoms. These complex anions are each surrounded by 9 La atoms located at the vertices of a tricapped trigonal prism (Fig. 3b). The filled prisms are stacked along the c axis sharing common triangular faces, thus forming an arrangement of infinite chains. Six chains around a sixfold axis are further connected via common faces to form a host framework containing hexagonal channels of carbon octahedra (Fig. 4). In total, the host framework contains two crystallographically independent Fe atoms at $4f$ (Fe1) and $2d$ (Fe2), two La atoms at $12i$ (La1) and $6h$ (La2) sites, and four C atoms at $2 \times 12i$ (C1, C2) and $2 \times 6h$ (C3, C4). All these sites are fully occupied and form a partial structure with chemical composition La_3FeC_6 . The remaining La atoms (La3, La4) are both located at $4e$ sites within the hexagonal channels. The total

Table 3

$\text{La}_{3.67}[\text{Fe}(\text{C}_2)_3]$: anisotropic displacement parameters U_{ij} [10^4 pm^2] ($f_{T, \text{anis}} = \exp[2\pi^2 \cdot (U_{11} \cdot h^2 + U_{22} \cdot k^2 + U_{33} \cdot l^2 + U_{12} \cdot h \cdot k + U_{13} \cdot h \cdot l + U_{23} \cdot k \cdot l \cdot b^* \cdot c^*)]$); estimated standard deviations are given in parentheses.

Atom	U_{11}	U_{22}	U_{33}	U_{12}	U_{13}	U_{23}
La1	0.0108(2)	0.0078(2)	0.0081(2)	0.0048(2)	0.0003(1)	-0.0001(2)
La2	0.0089(3)	0.0108(3)	0.0083(3)	0.0062(2)	0	0
La3	0.0073(3)	0.0073(3)	0.0161(7)	0.0037(2)	0	0
La4	0.0094(4)	0.0094(4)	0.0127(6)	0.0047(2)	0	0
Fe1	0.0067(4)	0.0067(4)	0.0091(7)	0.0034(2)	0	0
Fe2	0.0065(7)	0.0065(7)	0.0130(12)	0.0032(3)	0	0
C1	0.023(4)	0.027(5)	0.004(3)	-0.012(4)	0.001(3)	0.001(3)
C2	0.008(3)	0.012(3)	0.014(3)	0.004(3)	-0.009(3)	-0.007(3)
C3	0.007(4)	0.009(4)	0.012(5)	0.001(4)	0	0
C4	0.006(4)	0.007(4)	0.005(4)	0.000(4)	0	0

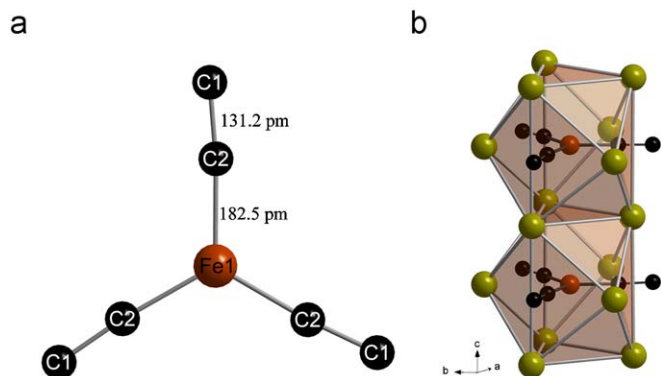


Fig. 3. The coordination around Fe. Fe1 shown as a representative: (a) the trigonal planar complex $\text{Fe}(\text{C}_2)_3$; (b) two tricapped trigonal prisms sharing common faces with La at the vertices enclosing the trigonal planar groups $\text{Fe}(\text{C}_2)_3$; the prisms form infinite chains along the c axis.

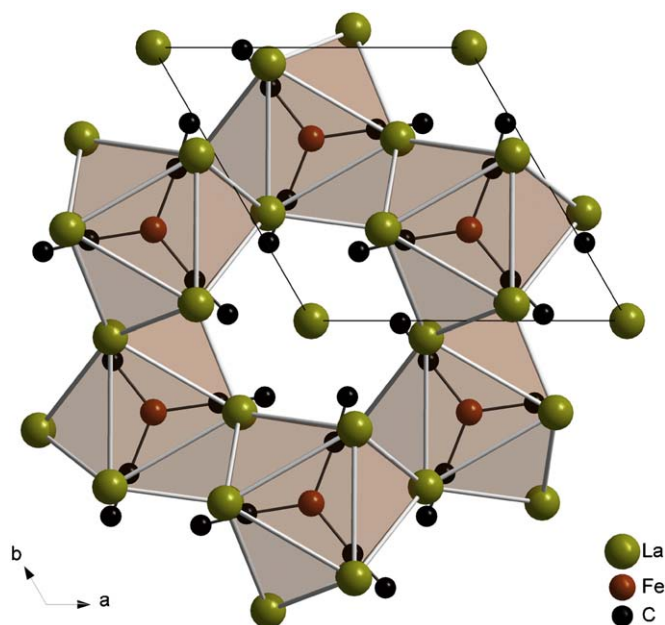


Fig. 4. Projection of the crystal structure viewed along the c axis showing the hexagonal channel stuffed by La3 and La4 atoms.

number of La atoms (La3 and La4) is four per supercell or $\frac{4}{3}$ La per subcell. When comparing the host structure in the previously reported subcell [1] and the supercell of the present work, the only difference is given by minor atomic displacements.

Therefore, the superstructure reflections mainly carry information on the arrangement of the La atoms accommodated inside the channels and thus we will consider only this part of the structure in detail. Fig. 5 shows different arrangements of the La atoms at $0, 0, z$ along the c axis. With respect to the substructure, i.e., folding back the superstructure (Fig. 5a), the La3 and La4 atoms would occupy split positions with $\frac{1}{3}$ probability at a $4e$ site of the space group $P6_3/m$. This is the highest possible site occupancy factor corresponding to the maximum La content because only every third position at $0, 0, z$ can be occupied due to distance constraints. Witte and Jeitschko [1] obtained a site occupancy factor of 0.32(3) from the refinement of the corresponding La position (La2 at $4e$ in Table 3 of [1]). This occupancy yields a composition $\text{La}_{3.64}\text{FeC}_6$. However, the authors decided to set the occupancy factor to the maximum value of $\frac{1}{3}$.

In the superstructure of the present work with the triple cell the two La sites, La3 and La4, are occupied with 50% probability each (Fig. 5b), which again results in a maximum La content, $\text{La}_{3.67}\text{FeC}_6$. Even in this supercell occupational disorder is still present. In case of a simultaneous occupation of neighboring sites the arrangement of La atoms along the chains would result in too short La–La distances. A chain of La atoms at maximum content is a priori determined by choosing a “start atom” and then extending the chain to infinity. Two different orientations with respect to the host structure are possible, here denoted as + and – (see Fig. 5c). Both chains have the same local environment, thus interchain interactions will determine the orientation of all chains. Because the interchain distance of 879 pm is quite large, significant interactions between the chains are not expected. Therefore, one can assume that the orientations of the chains are in this case uncorrelated, giving rise to the observed split atom density. In case that every second chain runs in opposite (–/+) direction (Fig. 5c), the average electron density is consistent with the obtained superstructure model given in Fig. 5b. Long range order of the chains would lead to a symmetry-breaking, which has not been observed. For example, a ferromagnetic-like correlation

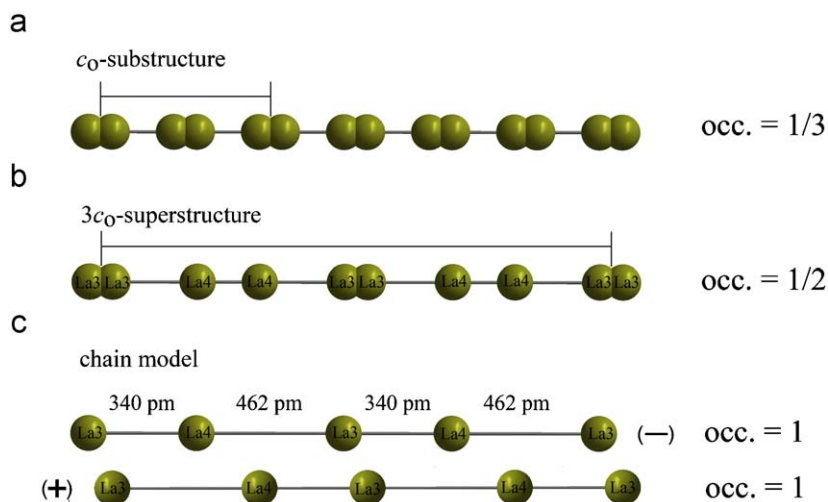


Fig. 5. Different arrangements of La atoms in the hexagonal channels running along the c axis: (a) split atom model of the substructure; (b) split atom model of the superstructure; this model is interpreted as a superposition of ordered chains as shown in (c): sequence of La atoms (La3, La4) with alternating short and long distances for two chains running in opposite ($-/+$) directions.

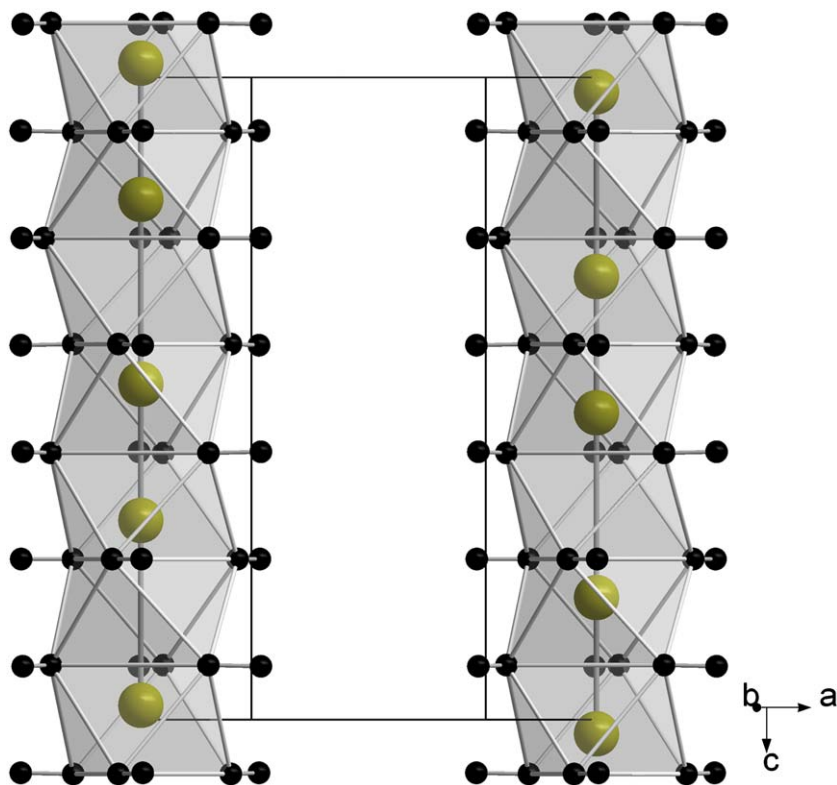


Fig. 6. Two chains of face-sharing carbon octahedra enclosing the La chains (La at $0, 0, z$) in $+$ and $-$ directions. Within each chain pairs of La atoms occupying positions out of the centers of two neighboring carbon octahedra alternate with one empty octahedron.

(++++...) would result in a simple ordered arrangement in the space group $P6_3$, whereas antiferromagnetic-like correlations would give rise to a more complex problem. In the case of long range order additional superstructure reflections must appear indicating even larger supercells. One can even anticipate complex domain structures. In general, the problem is similar as discussed for a triangular lattice Ising antiferromagnet.

The ordered chain model as shown in Fig. 5c indicates a Peierls-like distortion of the La-chains, yielding physically favorable distances. This is more clearly shown in Fig. 6. Here, two La-chains run antiparallel with the La atoms surrounded by

carbon octahedra. Within each chain pairs of La atoms occupying positions out of the centers of two neighboring carbon octahedra alternate with one empty octahedron.

As pointed out already, the chemical composition $\text{La}_{3.67}\text{FeC}_6$ represents the La-rich border of the compound. Higher La contents would result in too short La–La distances. The volume per formula unit of $\text{La}_{3.67}\text{FeC}_6$ with the triple cell is larger by about 1 \AA^3 than the volume reported by Witte and Jeitschko [1]. for the subcell. This small volume discrepancy together with the slightly smaller occupancy factor and the not observed superstructure (triple cell) indicate a possible La deficiency in the crystal

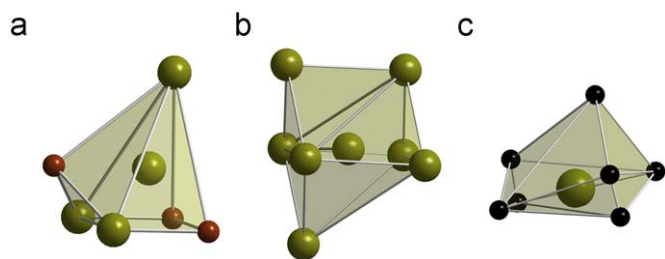


Fig. 7. Coordination polyhedra around La: (a) mono-capped square pyramid (coordination of La1 and La2) formed from three La and three Fe; (b) mono-capped distorted octahedron (coordination of La3 and La4); (c) $\text{La}(\text{C}_2)_2\text{C}_3$ square pyramid (coordination of La1 and La2).

investigated by Witte and Jeitschko. Indeed, in case of high quality crystals and at maximum La content one should observe the triple cell. However, a lower La content offers the possibility to arrange La atoms and vacancies in a disordered way within the chains, which then gives an additional contribution to the entropy of the system.

The coordination polyhedra around La are shown in Fig. 7. La1 and La2 are surrounded by six metal atoms (3 La and 3 Fe; Fig. 7a) forming a distorted mono-capped square pyramid. La3 and La4 are coordinated by seven La atoms in the form a mono-capped distorted octahedron (Fig. 7b).

The La–La distances vary between 340.34 and 372.68 pm which is slightly smaller than 366–377 pm observed in the different modifications of the pure metal [10–13]. The La–Fe distances are quite large (321.9–358.47 pm), slightly longer than observed in the crystal structure of $\text{La}_2\text{Fe}_{14}\text{C}$ [17] (306.4–339.5 pm). The La1 and La2 atoms have seven carbon neighbors, with $d_{(\text{La}1-\text{C})} = 265.73\text{--}281.53$ pm and $d_{(\text{La}2-\text{C})} = 273.45\text{--}286.48$ pm, respectively, (Fig. 7c). These distances are slightly shorter than $d_{(\text{La}-\text{C})} = 268.6\text{--}297.3$ pm in the crystal structure of La_2C_3 . The Fe–C distances at 182.47–183.65 pm are close to the respective values in the crystal structures of $\text{Ho}_2\text{Fe}_{17}\text{C}$ [14] ($d_{(\text{Fe}-\text{C})} = 175.7\text{--}191.7$ pm), $\text{Th}_4\text{Fe}_{34}\text{C}_3$ [15] ($d_{(\text{Fe}-\text{C})} = 191.4$ pm), Er_2FeC_4 [4] ($d_{(\text{Fe}-\text{C})} = 196.8$ pm), $\text{Lu}_2\text{Fe}_{14}\text{C}$ [16] ($d_{(\text{Fe}-\text{C})} = 198$ pm), and $\text{La}_2\text{Fe}_{14}\text{C}$ [17] ($d_{(\text{Fe}-\text{C})} = 203.5\text{--}219.8$ pm). The C–C distances (129.4 and 131.18 pm) are close to the respective value in ethylene (134 pm).

Assuming double bonds for the C_2 -pairs, the electropositive La donates all valence electrons to the $[(\text{FeC}_2)_3]$ polyanions. Without significant metal–metal interactions one may assign the oxidation state +1 for Fe: $\text{La}_{0.67}^{\text{III}}\text{La}_3^{\text{III}}[\text{Fe}(\text{C}_2)_3]^{4-}$. General formulae giving the overall stoichiometry of the compound are $\text{La}_{3.67}\text{FeC}_6$ or $\text{La}_{11}\text{Fe}_3\text{C}_{18}$. Suitable functional formulae are $\text{La}_{3.67}[\text{Fe}(\text{C}_2)_3]$ or $\text{La}_{11}[\text{Fe}(\text{C}_2)_3]_3$ with the square brackets denoting the anionic complex and the parentheses defining the ligands. A formula like $\text{La}_{0.67}\text{La}_3[\text{Fe}(\text{C}_2)_3]$ can be used to indicate the special nature of the La atoms at the 4e site. We have chosen here the formula $\text{La}_{3.67}[\text{Fe}(\text{C}_2)_3]$ because it is short and combines compositional as well as structural information.

4. Conclusion and summary

The ternary carbide $\text{La}_{3.67}[\text{Fe}(\text{C}_2)_3]$ with maximum possible La content forms a superstructure with a tripled unit cell along the c axis compared to the previously reported crystal structure [1]. The rigid host structure without any occupational disorder and with chemical composition La_3FeC_6 is identical for the sub- and super-structure (neglecting minimum distortions) and contains $\text{Fe}(\text{C}_2)_3$ trigonal planar groups with C_2 ligands bonded end-on to the iron atoms. These complex entities are surrounded by La atoms forming a framework of face-sharing tricapped trigonal

prisms. The resulting hexagonal channels of the host structure are occupied by additional La atoms at 0, 0, z with the maximum possible number of 4 atoms per supercell or $\frac{4}{3}$ atoms per subcell. Additional La atoms would result in too short interatomic distances. The chains are fully ordered and described in two different orientations (+, –). Disorder is still present in the superstructure due to the random alignment of neighboring chains. This results in split atoms each half-occupied by La at two 4e sites with respect to the supercell. The results are reported by Witte and Jeitschko [1] indicate the possible formation of at least a small number of vacancies, i.e., a small homogeneity range. The ordered arrangement of the La atoms at 0, 0, z shows a Peierls-like pattern with short and long distances. However, the driving force for this behavior is still unclear. The following questions remain open:

- What is the most stable ordered structure for the chemical composition $\text{La}_{3.67}[\text{Fe}(\text{C}_2)_3]$?
- What kind of interchain interactions are expected between neighboring chains: ferromagnetic- or antiferromagnetic-like?
- What is the driving force for the Peierls-like distortion for the chain of La atoms inside the channels?
- Does $\text{La}_{3.67}[\text{Fe}(\text{C}_2)_3]$ represent a “line compound $\text{La}_{11}\text{Fe}_3\text{C}_{18}$ ” or a phase with homogeneity range?
- What is the lower limit of the La content in case of a homogeneity range?
- Is it possible to substitute La atoms inside the channels by suitable other elements?
- Is it justified to assign of double bonds in case of the C_2 -pairs?
- Is it justified to consider isolated complex entities in case of the $[\text{Fe}(\text{C}_2)_3]$ units and to use the square brackets?

These questions will be addressed in a forthcoming paper.

Acknowledgments

We would like to thank Dr. Ulrich Burkhardt, Torsten Vogel, and Monika Eckert (metallographic investigations and EDXS) as well as Steffen Hückmann (X-ray powder diffraction).

References

- [1] A.M. Witte, W. Jeitschko, Z. Naturforsch. 51b (1996) 249–255.
- [2] E. Dashjav, G. Kreiner, W. Schnelle, F.R. Wagner, R. Kniep, W. Jeitschko, J. Solid State Chem. 180 (2007) 636–653.
- [3] J.D. Livingston, in: K.J. Strnat (Ed.), Proceedings of the Eighth International Workshop on Rare Earth Magnets and Their Application, Dayton, Ohio, 1985, p. 423.
- [4] M.H. Gerss, W. Jeitschko, L. Boonk, J. Nienstedt, J. Grobe, E. Mörsen, A. Leson, J. Solid State Chem. 70 (1987) 19–29.
- [5] R.-D. Hoffmann, R. Pöttgen, W. Jeitschko, J. Solid State Chem. 99 (1992) 134–139.
- [6] W. Jeitschko, M.H. Gerss, J. Less-Common Met. 116 (1986) 147.
- [7] R. Pöttgen, W. Jeitschko, U. Wortmann, M.E. Danebrock, J. Mater. Chem. 2 (1992) 633–637.
- [8] STOE WinXPow, Ver. 1.2 STOE & Cie. GmbH, Darmstadt 2001.
- [9] G.M. Sheldrick, SHELX97, Programs for the Solution and Refinement of Crystal Structures, University of Göttingen, Germany, 1997.
- [10] B.J. Beaudry, P.E. Palmer, J. Less-Common Met. 34 (1974) 225–231.
- [11] K.W. Herrmann, Iowa State Coll. J. Sci. 31 (1956) 439–440.
- [12] F.H. Spedding, J.J. Hanak, A.H. Daane, J. Less-Common Met. 3 (1961) 110–124.
- [13] G.J. Piermarini, C.E. Weir, Science 144 (1964) 69–71.
- [14] G. Bocelli, G. Calestani, Chem. Mater. 5 (1993) 129–131.
- [15] O. Isnard, J.L. Soubeyrou, D. Fruchart, T.H. Jacobs, K.H.J. Buschow, J. Alloys Compd. 186 (1992) 135–145.
- [16] C.J.M. Denissen, B.D. de Mooij, K.H.J. Buschow, J. Less-Common Met. 139 (1988) 291–298.
- [17] E.P. Marusin, O.I. Bodak, A.O. Tsokol, V.S. Fundamenskii, Kristallografiya 30 (1985) 581–583.